Bulgarian Chemical Communications, Volume 48, Special Issue G (pp.79-84) 2016

Two-wavelength lasers based on pumping by laser Gaussian-beam as instrumentation for materials and chemical products analysis

M. Deneva*

"QOE" Scientific Laboratory, R&D Dept., Technical University of Sofia and "OELE" Dept., TU-Branch Plovdiv, BG

Received October 10, 2016; Revised November 10, 2016

We have developed, as a tool for differential-absorption spectroscopy and two-photon study of materials and chemical products composition, effective lasers with two or more independently tunable wavelengths. Our solution is based on the idea to combine a standard laser Gaussian beam longitudinal pumping of lasers, especially of dye lasers, with patented by us multi-coaxial-channels laser geometry. The Gaussian beam, due to its unique intensity distribution in the cross section, creates in the pumped laser active medium high pumping in the axial part and low pumping in the periphery. These two parts are optically separated and each generates in its own spectrally selective resonator. Beside the competition-less generation at two independently controlled wavelengths, other specific and essential advantages of the proposal are: i) both emissions – at the weeker line, generated in the amplified curve wings, and at the stronger line - arround the maximum of amplification, are produced with equalized energy without loss of pump energy for the equalisation and simultaneously ii) the two emissions are produced and emitted naturally in coaxial beams using entire laser medium volume. We report general modelling and detailed theoretical analysis of such a laser action on the basis of Rhodamine Dye in ethanol, pumped by Gaussian beam of Nd:YAG laser (0.53 μm). We succesifully tested the new solution with its advantages. We applied the two-wavelength laser light as a tool in differential absorption spectroscopy (DAS) to detect the presence and to measure concentration of Nd^{3+}-ions in a material under investigation.

Keywords: tool for DAS, two-wavelength lasers, dye lasers, Gaussian beam pumping, two-coaxial channel laser geometry, DAS chemical composition study.

INTRODUCTION

Today various specialized laser instrumentation has become a perspective tool for studying composition of materials and chemical products. Widespread application is the Differential-Absorption Spectroscopy (DAS) for local and remote use, the last especially for study of gas components in the atmosphere [1, 2]. The DAS method is based on comparison of the passed or diffused light power at two laser wavelengths - one of them coinciding with a specific line of absorption and the other – with non-absorption parts of the spectrum. The development of this technique is closely related to development of specific lasers that produce emission at two (or more) independently tunable lines, i.e. the so called two-wavelength lasers. Such lasers find wide application also in general spectroscopy, in non-linear optics, in bio-medical investigations and treatments [3-5]. More detailed review of the two-wavelength lasers and their applications is given in the recent papers [6-8].

The aim of this work is to report a new and highly efficient two-wavelength laser. This includes the proposed principle, detailed theoretical description, test implementation and experiment to prove the potential of such a laser to find the presence and concentration of given atomic particles in a mixed substance. We employ a new idea to combine the standard longitudinal pumping of wideband amplification laser medium (in the work - laser dye) with a Gaussian laser beam and our coaxial multi-channel laser geometry [9, 6]. The Gaussian beam, due to its peculiar intensity distribution in the cross section, creates in the pumped cylindrical laser active medium high pumping (and high amplification) in the axial part and low pumping (low amplification) in the periphery. We can separate optically these two parts to generate in two different spectrally selective resonators. If in the high amplification axial part we generate at wavelength with low emission cross-section and at the periphery part – at wavelength with high cross-section and choose convenient diameters of the two volumes, we can generate the two lines with equal energy without

* To whom all correspondence should be sent:
E-mail: mar.deneva@abv.bg

introduction of any corrected additional losses in the channels. The two generations are without competition and are produced and emitted naturally in coaxial beams using entire laser medium volume. These advantages are unique for the proposal. Still more, the longitudinal pumping has as general advantages, in comparison with the transversal pumping, use of low concentration and a big diameter pumped region of the active medium, which lead to better homogeneity and lower divergence. In the work, firstly we described the proposed laser scheme, secondly we modeled and provided detailed theoretical and numerical analysis of the action of such new laser solution. We made succesiful tests of the new solution to show its advantages. As an application, we used the produced two-wavelength laser light as a tool in DAS and found the presence of the searched Nd^{3+}-ions and measured their concentration in a sample under investigation.

PRINCIPLE AND THEORETICAL ANALYSIS

Schematic of the proposed longitudinally pumped with a Gaussian beam two-wavelength coaxial-architecture laser is shown in Fig.1. The principle is described on the example of Rhodamine Dye in ethanol (concentration 2x10-4 mol/l), longitudinally pumped by Gaussian beam distribution, second harmonic (0.53 μm) of Nd:YAG laser (pump energy of ~25 mJ; pulse length of ~ 30 ns). The dye solution filled a cylindrical cell (noted as Dye AM – Active Medium) with length l and diameter d (5 mm and 6 mm, respectively). The input pump beam passes through lens with suitable focal length (0.6 cm) to form a spot at the input of the AM with a diameter of the pumped part of ~ 6 mm that contains ~ 99 % of the incident beam power P_{tot} (i.e. 1.6 times higher than the Gaussian radius of 3.75 mm on the AM input). The Rayleigh length is essentially larger than the length l of the cell, which permits to accept parallel propagation of the Gaussian beam in the AM. After the lens, a multichroic mirror M_{ref} tilted at ~30° is placed (reflectivity R ~0.9 for 0.54-0.6 μm, and ~ 0.1 for 0.53 μm). The laser output mirror M_{out} is also multichroic (R ~ 0.7 for 0.54 - 0.6 μm and ~ 0.1 for 0.53 μm). At the opposite end of the AM, a near-plane multichroic mirror M_{pb} with radius of curvature few meters (R ~ 0.1 for 0.54-0.6 μm and ~ 0.8 for 0.53 μm) is suitably adjusted The generation at the two wavelengths (scheme in Fig.1) is produced in two coaxially disposed and optically separated parts of the AM. A spectrally-selective resonator with length L (~ 5 cm) was formed for each part. The separation (hatched differently in Fig.1) is obtained using a dividing rectangular prism (DP), declined at a small angle (~5°) with respect to the cell axis to avoid the back Fresnel's reflection. The prism has a 0.3 cm diameter bored hole with length of 0.4 cm. In the hole a very thin (~0.1 mm wall) metal tube with 2 cm length is introduced, that assures very good separation of both channels as we have shown in our previous work [6]. The resonator for generation in the internal part (internal channel, generation at λ_i), built of M_{out} and M_i and the active volume, is separated by the tube through the prism. The spectral selection is done by the Interference Wedge IW_i [10] with thickness of 6 μm, reflectivity of the layers ~0.9 and apex angle of 5.10^{-5} rad that assures tunable selection in the amplification range of the generated dye and with linewidth ~ 0.3 nm. The external part (external channel, λ_e) generates in the resonator formed by M_{out}, internal reflection by the prism DP and selector combination of 1200 l/mm Diffraction Grating DG_e and the plane mirror M_e providing tunable selection with linewidth of ~ 1 nm in the gain region of the AM. We will use below the given already parameters of the laser construction.

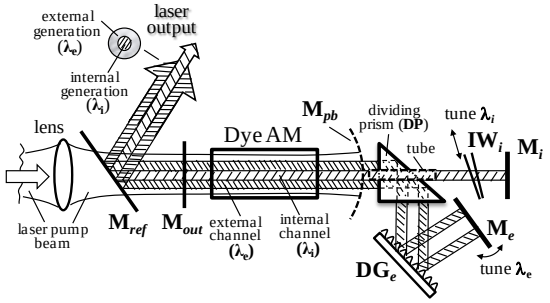

Fig. 1. Optical scheme of the laser with channels dividing prism DP with a hole.

THEORETICAL MODELLING

Theoretical analysis aims to obtain the conditions – especially AM separation in combination with the wavelength shift, for which simultaneous generation is possible with near equal output energies. We will consider the important, however difficult case, when one line is near the maximum of the amplification gain, and the second - shifted far from the maximum. In the common volume for lasers with homogeneously broadened amplification (our case), due to the so-called "wavelength competition" effect [11, 12], the generation of the weaker line is completely suppressed by the stronger one.

Firstly, in the theoretical analysis, we have calculated the pumped power distribution in the AM. For the used Rh6G dye concentration from the measurement, we have evaluated the non-saturated absorption coefficient for the pump 0.53 μm light to be ~ 12 cm^{-1}. The approach applied by us is schematically clarified in Fig.2. AM is divided radially into rings and longitudinally - in slices. The cross section of the cell is divided at 7 rings with equal increasing radii for each sequent by Δr (see Fig.2b). Along the axis Z of the crystal the division is at 5 slices each with equal length $\Delta l = l/5$. We have Δl =0.1 cm and Δr = 0.042 cm.

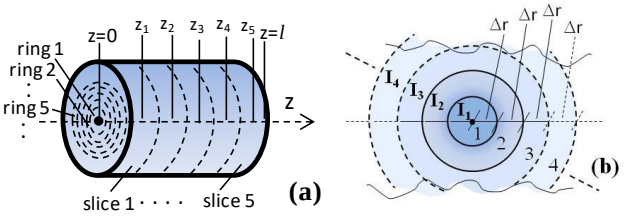

Fig. 2. Schematic dye cell division: **(a)** longitudinally in slices and **(b)** radially in rings

The Gaussian pumping (radius 3.75 mm) is with 25 mJ in ~30 ns pump pulse. The input beam is centered on the AM axis. Let's first consider the distribution of the pumping for each cylinder formed by border lines parallel to the axis of the dye cell and closed by the pair of rings at the front and rear sections of the dye cell (partial cylinders). The maximal intensity I_0 in the center of the beam at the entry plane of the dye cell was calculated on the base of well-known relation:

$$I_0 = \frac{2P^{\max}}{\pi \cdot \omega^2} \qquad (1)$$

where $P^{\max}$ is the maximal pump power in the pulse and ω is the Gaussian radius of the pump beam. The intensity for each partial cylinder is calculated at the middle of the ring radius ($r_i = (2 \cdot i - 1) \cdot (\Delta r/2)$, $r = 1, 2 \ldots 6$) and is assumed to be homogeneous for the ring. The points on the graphics in Fig.3 present the values for the corresponding rings.

The distribution of the pump power for each ring and starting pump intensity are presented in Fig.3(b). In the calculations for propagation along the Z axis, we have used the Bouger's law, taken into account the effect of absorption saturation. We have evaluated the change of the pump intensity correspondingly for each ring, slice by slice – forward and backward after reflecting by the mirror M_{pb}. For each slice we sum forward and backward values, accepting that for any ring of the slice the intensity is constant, equal to this one at the half length of the slice. We assume a total input in the crystal pump power $P_{tot} \approx 25$ mJ / 30 ns at Gaussian beam intensity distribution.

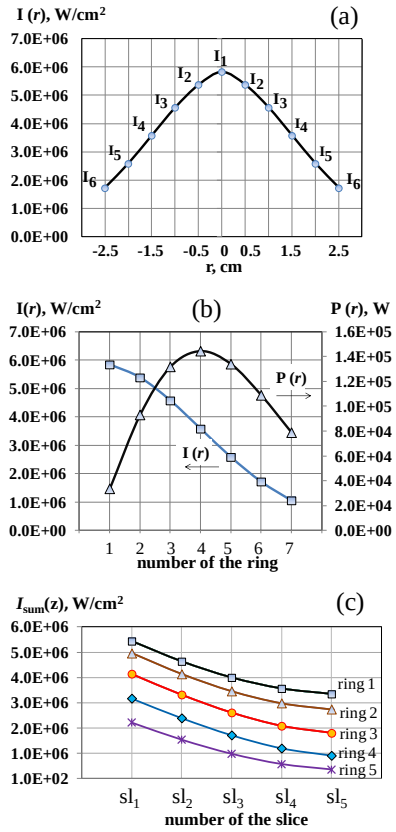

Fig.3. **(a)** Calculated distribution of the pump intensity (I_i) in the cross section; **(b)** The pumping power P(r) corresponding to each ring; **(c)** The result pump intensity for the first five rings (the axis X shows the number of the slice sl_i, i=1,2..5).

In Fig. 2(a) z_i (i = 1, 2, …5) corresponds to the middle of the slice length, where the result intensity is calculated. The values of the obtained intensity I_{r,z_i} for the first five rings, after summing the forward and backward values, calculated slice by slice are presented in Fig.3(c). The calculated plots in this figure show for each partial cylinder, with acceptable accuracy, the sum pump power (and energy) to be uniform both in slices and in the cross section – i.e. in the corresponding ring. This uniformity determines the fact that we can accept homogeneity of the pumping with different energy density for the partial cylinders. The change in the intensities from the first to the last slice for the corresponding cylinder is of the order of a few percents and practically could be taken as constant for each ring. On this base, we can calculate the generation for each partial cylinder applying the set of rate differential equations [11] adapted for the

case, presented in the next point. The considerable difference in the pump power for the cell parts around the axis and in the peripheral areas makes possible generation at weaker lines (with smaller values of the emission cross-section) comparable to that at the stronger lines, when they are generated in peripheral part of the dye cell. We show this possibility for the wavelength 594 nm, generated in near axial part and the wavelength 558 nm generated in the peripheral part of the cell.

ANALYSIS OF THE LASER GENERATION

Taking the approximately constant value of the pump energy into slices along the axis of the crystal – i.e. possibility to assume homogeneity of excitation (with different energy density for the corresponding ring), we apply the adapted set of differential rate equations [11] for the analysis. The adapted system that describes our case at assumed parameters is:

$$\frac{dN_2}{dt} = R_p^{(e,i)}(t) - B^{(e,i)} \cdot q^{(e,i)} \cdot N_2 - \frac{N_2}{\tau}$$
$$\frac{dq^{(e,i)}}{dt} = Va^{(e,i)} \cdot B^{(e,i)} \cdot q^{(e,i)} \cdot N - \frac{q^{(e,i)}}{\tau_c^{(e,i)}} \qquad (2)$$

with $P_{out}^{(e,i)}(t) = \left(\gamma_{out}^{(e,i)} \cdot c / 2L'\right) \cdot h\nu^{(e,i)} \cdot q^{(e,i)}(t)$ (3)

Here $B^{(e,i)} = \sigma_{21}^{(e,i)} \cdot l \cdot c / V_a^{(e,i)} \cdot L'$ s^{-1};

$\sigma_{21}^{(e)} = 2\times10^{-16}$ cm^2; $\sigma_{21}^{(i)} = 1.14\times10^{-16}$ cm^2 – emission cross-section of the Dye laser medium for λ_e = 558 nm and λ_i = 594 nm [11], l – dye cell length; c = 3×10^{10} cm/s is the light velocity; L' = 6.7 cm is the optical length of the resonator. The lifetime of the upper laser level is τ = 3 ns. The term in (3) $h\nu^{(e,i)} \sim 3.3\text{x}10^{-19}$ J is the energy of the generated photons for the corresponding wavelength. The dumping time of the photon in the resonator is $\tau_c^{(e,i)} = L' / c \cdot \gamma^{(e,i)}$, where $\gamma^{(e,i)}$ describes the losses in the respective resonator following Ref. [11] accounting the corresponding considered ring (partial cylinder). The calculations are for the laser and pumping parameters, given already. The total number of active Rh6G molecules cm^3 used in the calculations is 1.2×10^{17} cm^{-3} ($2\text{x}10^{-4}$ mol/l Rh6G). The pump rate $R_p^{(e,i)}(t) = P_p^{(e,i)}(t) / \left(h \cdot \nu^{(e,i)}\right) \cdot V_a^{(e,i)}$ is defined on the base of the part of the optical pumping power that corresponds to the considered ring and wavelength. According our data, the obtained pump power for each ring can be determined from Fig.3. The pump power is a function of the area and the intensity in the ring. $R_p^{(e,i)}$ is related to the temporal shape of pump energy in combination with the laser pump pulse shape. The Q-switched laser pump pulse can be well approximated by a trapezoid shape with a rise time of 10 ns, near-plateau part of 10 ns and fall time of 30 ns. $V_a^{(e,i)}$ is the active volume of the considered ring for the generation of the corresponding wavelength. In the calculations we have taken the geometrical data for each ring derived from the description of the laser cell separation given above.

The system (2-3) is solved using the Runge-Kutta method independently for the generation in each considered coaxial part – for each cylinder, with initial conditions N = 0 and $q^{(e,i)} = 1$. Solution of the system gives the temporal shapes of the laser outputs and their integration [11] is the output energy. For the used parameters, generation in six rings in total is obtained – in the first three rings the 594 nm wavelength is generated, and for the next three rings generation for the 558 nm wavelength is produced. Typical plots for generation at 594 nm (rings 1+2+3) and at 558 nm (rings 4+5+6) are presented in (Fig.4a). The plot modulation at 558 nm we relate to the small number of the rings, however this fact does not change essentially the real temporal shape of the laser emission at this wavelength, as shows the experimental results. The output energy for the wavelengths for the corresponding partial cylinder is plotted in Fig.4(b). The calculations show also that both generations are temporally superimposed with some difference of the starting of each generation of order of 5 ns.

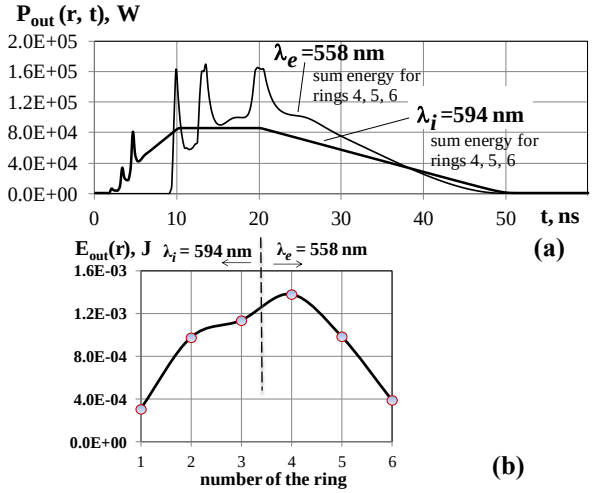

Fig. 4. (a) Temporal generation at λe = 558 nm (1+2+3 rings) and at λi = 594 nm (4+5+6 ring), respectively; **(b)** Calculated output energy in rings 1, 2, 3 (at λ_i = 594 nm) and in rings 4, 5, 6 (at λ_e = 558 nm).

The total output energy produced at 594 nm is ~ 2.5 mJ and at 558 nm ~ 2.8 mJ. Thus it is really possible to obtain practically equal energetic characteristics of both generations. For generation in a single common volume, the lasing at 558 nm suppresses the lasing at 594 nm.

THE EXPERIMENTAL TEST

The analysis in the previous section, besides showing the feasibility of our proposal with its advantages, confirms that the chosen parameters are well suitable for such laser realization. We have realized the laboratory prototype of the laser with elements and pumping parameters close to those in the previous section. To realize the DAS testing experiment, the two wavelengths are tuned to be at 561 nm (λ_e) and 579.6 nm (λ_i), with energy ratio ~ 1:0.6. The sum output at these two wavelengths (for our non-completely optimized test laser), was ~ 1.6 mJ that easily can be decreased using filters. The tuning in the range of ~ 6 nm conserves the two generations with acceptable equality of ~ 1:0.6 at the optimum (our case) to 1:0.3 at the ends. Both generations are emitted in coaxial beams, each with similar cross-section distribution to the spot of two-coaxial beam emission of a solid-state laser, shown in our work [6]. The internal beam has a circular ~3 mm diameter spot and the external - a ring one.

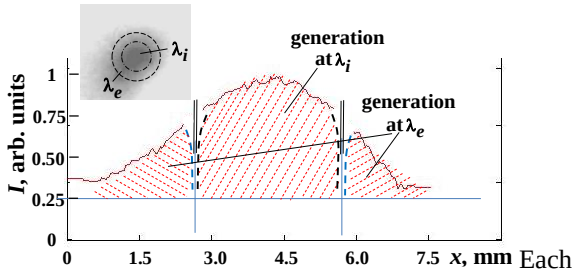

Fig. 5. The curve of spatial distribution of the two-wavelength laser output and the actual photograph –in the inset.

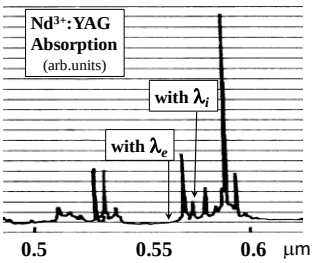

Fig. 6. The parts of the absorption spectrum of Nd^{3+}-ions in the YAG crystal and the wavelengths of the illuminating laser beams [13].

Each beam can be presented as superposition of few transversal modes [6], for internal – TEM_{00} + TEM_{01*} and for the external – of two cylindrical modes of type TEM_{04}, turned radially with respect to each other at $\pi/8$ (each mode has maximums in the minimum-holes of the other). The external boundary of the internal spot and the internal boundary of ring-spot of the external beam, at some distance (of ~ 1.5 m) from the laser output, merge due to diffraction. The spots of the two-wavelength generation are shown in Fig.5.

We demonstrate the two-wavelength DAS spectroscopy method, using the two-wavelength laser for evaluation of Nd^{3+}-ions concentration in Nd^{3+}:YAG crystal. The part of the absorption spectrum of Nd^{3+}-ions is shown in Fig.6 [13]. The wavelength at λ_e coincides with the absorption minimum (practically zero) at 561 nm and the other - λ_i - with the absorption line (with $\sigma_{ab}=0.54\text{x}10^{-20}\text{cm}^{-1}$ [11]). When the light at these two wavelengths passes through the crystal sample with length ξ, decreasing of intensity at each wavelength is different. We can write for our case for the decreased power of the incident intensities $I_0^{e,i}$ (W/cm^2), that is adjusted to be less than 25 kW/cm^2 (saturation intensity for Nd^{3+}), for non-saturated transmission $I_{pas}^{i} = I_0^{i} \cdot e^{-\left(\sigma_{ab}^{i} \cdot N \cdot \xi + \alpha \cdot \xi\right)}$ at λ_i, $I_{pas}^{e} = I_0^{e} \cdot e^{-(\alpha \cdot \xi)}$ at λ_e. Here α, in cm^{-1}, is the coefficient of light decreasing due to different reasons, common for both wavelengths – reflection at the sample input and output surfaces, scattering, non-spectral selective absorption of impurities. After some simple calculation, we have:

$$N = -\left(\sigma_{ab}^{i}\right)^{-1} \xi^{-1} \cdot \ln\left[\left(I_{pas}^{i}/I_0^{i}\right)\cdot\left(I_{pas}^{e}/I_0^{e}\right)^{-1}\right] \qquad (4)$$

In our case, from the easily measured ratios $\left(I_{pas}^{i}/I_0^{i}\right)$=0.042 and $\left(I_{pas}^{e}/I_0^{e}\right)$=0.64, at σ_{ab}^{i} = $0.52\text{x}10^{-20}$ cm^2 [13] and ξ =8 cm, the concentration of Nd^{3+}-ions is $6.4\text{x}10^{19}$ cm^{-3}.

CONCLUSION

In the work we have shown – theory and the experimental test - the possibility to use the specific light intensity pump beam distribution in the Gaussian beam in combination with special coaxial geometry to obtain a new two-wavelength laser. This laser, beside the absence of non-desired wavelength-competition effect [12, 14], assures laser emission simulataneously at tunable weak and strong lines with practically equal energies without loss of pump energy for the equalisation. The two emissions are produced and emitted naturally in coaxial beams using the entire rod volume. Such

lasers can be considered as an effective tool in differential absorption spectroscopy in chemical analysis. Confirming experimental test, using the two-wavelength light to detect the presence and concentration of Nd^{3+}-ions in mixed substance, is also given.

REFERENCES

1. W. Demtröder, Laser spectroscopy: basic concept and instrumentation, 3th ed., Springer, (2003).
2. V. Vaicikauskas, Z. Kuprionis, M. Kaucikas, V. Svedas, V. Kabelka, *Proc. of SPIE*, **6214**, 62140E (2006).
3. M. L. Rico, J. L. Valdes, J. Martinez-pastor, J. Capmany, *Optics Communs.*, **282**, 1619 (2009).
4. L. Zhao, J. Su, X. Hu, X. Lv, Z. Xie, G. Zhao, P. Xu, S. Zhu, *Opt. Express*, **18**, 13331 (2010).
5. B. Devaux, F. Roux, Acta Neurochirurgia, the Eur. J. Neurosurgery, **138**, 1135 (1996) and the literature cited there in.
6. M. Deneva, M. Nenchev, E. Wintner, S. Topcu, *Opt. Quant. Electron.*, **47**, 3253 (2015).
7. A. Sato, Sh. Okubo, K. Asai, Sh. Ishii, K. Mizutani, N. Sugimoto, *Appl. Opt.*, **54**, 3032 (2015).
8. Y. G. Bassov, *Sov. J. Appl. Spectr.* (ed. USA), **49**, 6 (1989).
9. M. N. Nenchev, *BG patent* IIR 25954 (1978).
10. E. Stoykova, M. Nenchev, *JOSA*, **27**, 58 (2010),
11. O. Svelto, Principles of lasers, 5th ed. Springer Science+Business Media, LLC 2010 (2010).
12. Y. Louyer, J. Wallerand, M. Himbert, M. Deneva, M. Nenchev, *Appl. Opt.*, 42 (27), 5463 (2003).
13. W. Koechner, Solid-State Laser Engineering, 6 revised and updated edition, Springer, Berlin (2005).
14. M. Deneva, P. Uzunova, M. Nenchev, *Opt. Quant. Electron.*, **39**, 193 (2007).

ДВУВЪЛНОВИ ЛАЗЕРИ, БАЗИРАНИ НА ЛАЗЕРНО ВЪЗБУЖДАНЕ С ГАУСОВ СНОП КАТО ИНСТРУМЕНТАРИУМ ЗА АНАЛИЗ НА МАТЕРИАЛИ И ХИМИЧЕСКИ ПРОДУКТИ

М. Денева

Лаборатория „Квантова и оптоелектроника", НИС, Технически университет София и Катедра „Оптоелектронна и лазерна техника" – ТУ-Ф-л Пловдив;

Постъпила на 10 октомври 2016 г.; коригирана на 10 ноември, 2016 г.

(Резюме)

В работата ние предлагаме нов атрактивен двувълнов лазер, отнасящ се към важните инструменти за спектрален анализ на състава на материали и химически продукти с техниката на диференциално-абсорбционна спектроскопия (ДАС) и дву-фотонно третиране. Нашето решение се основава на нова идея да се комбинира надлъжно възбуждане на лазер, особено багрилен лазер, чрез стандартен Гаусов лазерен сноп с нашата патентована мулти-коаксиална геометрия на каналите в лазера. Гаусовият сноп, поради специфичното разпределение на интензитета в напречно сечение, създава във лазерната активна среда високо възбуждане в аксиалната й част и ниско възбуждане в нейната периферия. В нашето решение, тези две части оптически са разделени коаксиално и всяка генерира в свой собствен спектрално – селективен резонатор. Освен генерация на две независимо управляеми дължини на вълната без конкуренция, други специфични предимства на предложението са: 1). двете генерации – на слабата линия, генерирана в краищата на спектралната крива на усилване, и на силната линия – около максимума на спектрално усилване на средата, се произвеждат с приблизително еднаква (изходна) енергия без загуба на възбуждаща енергия за изравняването им, и едновременно; 2). двете генерации се произвеждат и генерират естествено в коаксиални снопове, използвайки целия лазерен обем на средата. Ние представяме обобщено моделиране и детайлен теоретичен анализ на действие на този нов лазер, с използването на числено обсъждане на родаминово багрило в етанол, възбуждано от Гаусов сноп от Nd:YAG лазер (0.53 μm) и успешно сме тествали новото решение с неговите предимства. Като приложение, използвайки двувълновата лазерна светлина като инструмент в ДАС, ние показваме присъствието на Nd^{3+}-йони и измерихме концентрацията им в изучаван материал.